View metadata, citation and similar papers at core.ac.uk
brought to you by CORE
provided by Elsevier - Publisher Connector

Engineering 2015, 1(2): 234–242
DOI 10.15302/J-ENG-2015040

Research

Advanced Materials and Materials Genome—Article

High-Throughput Screening Using Fourier-Transform Infrared Imaging

Erdem Sasmaz, Kathleen Mingle, Jochen Lauterbach*

ABSTRACT Efficient parallel screening of combinatorial libraries is one of the most challenging aspects of the high-throughput (HT) heterogeneous catalysis workflow. Today, a number of methods have been used in HT catalyst studies, including various optical, mass-spectrometry, and gas-chromatography techniques. Of these, rapid-scanning Fourier-transform infrared (FTIR) imaging is one of the fastest and most versatile screening techniques. Here, the new design of the 16-channel HT reactor is presented and test results for its accuracy and reproducibility are shown. The performance of the system was evaluated through the oxidation of CO over commercial Pd/Al_2O_3 and cobalt oxide nanoparticles synthesized with different reducer-reductant molar ratios, surfactant types, metal and surfactant concentrations, synthesis temperatures, and ramp rates.

KEYWORDS high-throughput, FTIR imaging, screening, cobalt oxide, CO oxidation

1 Introduction

Catalysis has had a tremendous impact on the chemical industry over the last century. It has been estimated that 90% of chemicals are derived from catalytic processes [1] and about 90% of these processes include heterogeneous catalysis [2]. Despite the large number of catalytic processes, the discovery and deployment of advanced materials from laboratory to application often take a considerable amount of time, typically requiring 10–20 years, and often relying on trial and error [3].

High-throughput experimentation (HTE) has been shown to accelerate the discovery and development of new catalyst formulations and routes for desired products, while optimizing reaction conditions. Since the early 1980s, HTE methodologies have been shown to improve the success of research and development (R&D) through the rapid synthesis and screening of large material libraries [4–9]. HTE methodologies are capable of generating large datasets and populating material properties and catalytic activities. However, existing HTE methodologies suffer from the lack of a widespread adaptation of standards for materials synthesis, characterization, and data management. In 2011, the Materials Genome Initiative (MGI) was launched by the US government to accelerate the discovery, development, and deployment of advanced materials, while reducing the cost of R&D [10]. In order to enhance the adaptation of standards and to positively impact material discovery and commercialization, one of the objectives of the MGI is to facilitate the sharing of HTE tools. This is done by creating a searchable online database for large library sizes and establishing HTE centers with on-site synthesis, screening, and characterization capabilities [10].

Generating a common high-throughput (HT) database requires the effective implementation of combinatorial workflows consisting of experimental design, material synthesis, material characterization, and data collection processes [11]. The Dow Chemical Company, for example, has successfully implemented HT workflow through several automated syntheses, testing units, and HT characterization tools. In a recent study, they have shown that over 1000 catalysts were synthesized and tested for their activity in propane oxidative dehydrogenation [4]. The data obtained from each workflow step is stored in a single database in order to effectively screen materials and speed up the development process, which fits well with the objective of the MGI [4]. In addition to the establishment of an effective combinatorial workflow, successful catalyst evaluation can be divided into a series of steps that include a primary screening to discover promising materials for the application of interest; a secondary, more detailed investigation of the selected materials from the primary screening; and subsequent scaling-up and commercial testing [5]. Previously in our group, HT screening methodologies were successfully applied to identify novel catalyst formulations for the catalytic cracking of military jet fuel (JP-8) to liquefied petroleum gas. The approach combined a rapid, qualitative primary optical screen via thin-film techniques,

SmartState Center for Strategic Approaches to the Generation of Electricity (SAGE), Department of Chemical Engineering, University of South Carolina, Columbia, South Carolina 29208, USA
* Correspondence author. E-mail: lauteraj@cec.sc.edu
Received 8 June 2015; received in revised form 26 June 2015; accepted 30 June 2015

© The Author(s) 2015. Published by Engineering Sciences Press. This is an open access article under the CC BY license (http://creativecommons.org/licenses/by/4.0/)

a series of quantitative screens using milligrams of powder catalysts, and a final verification of the best samples using a single-sample reactor [12].

Although HTE methodologies have been effectively used to screen catalyst formulations, the implementation of combinatorial approaches to the development of heterogeneous catalysis remains a challenge due to the dynamic nature of the catalyst material. The performance of a catalyst typically depends on many parameters associated with its structure, composition, synthesis conditions, and deactivation, as well as the binding strength of reactants and products of interest [12–15]. The optimization of this parameter space could involve up to 3 000 000 parallel runs [9], which is not possible to complete even using state-of-the-art HTE methodologies. Both stochastic and deterministic methods have been proposed in order to reduce the size of the catalyst library and decipher the quantitative relationship between parameter space and catalyst activity. Of these methods, the most commonly used in HT analysis include design of experiments (DOE), artificial neural networks, and genetic algorithms. The details of these methods and their successful implementation to the HTE are described elsewhere [7, 16–22].

The challenges associated with the dynamic nature of the catalyst and the large parameter space of catalyst libraries can be overcome by developing sophisticated HT screening tools that can predict catalytic activity rapidly and accurately. Successful development of these tools often depends on the design of parallel reactors, reaction conditions, and the capability of analysis equipment. To date, most HT screening tools rely on optical, mass-spectrometric, and chromatographic techniques [9, 13, 23–25]. In the following section, the details of several of these techniques are discussed briefly. In addition, the Fourier-transform infrared (FTIR) imaging developed in our group is described and compared with state-of-the-art HT screening tools.

2 Brief overview of methodologies for the screening of heterogeneous catalysis

Optical screening techniques in HTE include infrared (IR) thermography, cataluminescence (CTL), laser-induced fluorescence imaging (LIFI), resonance-enhanced multiphoton ionization (REMPI), and FTIR. Early studies have applied IR thermography to determine catalyst activity based on the radiation energy emitted by the catalyst surface. Radiation energy is highly sensitive to the temperature on the catalyst surface, such that small temperature variations can be picked up by the detector. IR thermography therefore allows the catalytic activity of an exothermic reaction to be quickly screened. For example, Olong et al. have used emissivity-corrected IR thermography to screen catalysts for low-temperature soot oxidation [26]. The relative heats of the oxidation reactions of up to 207 catalysts were analyzed in parallel. Due to the unpredictability of intimate contact between soot and a catalyst, the accuracy of the data obtained in the HT analysis was validated by conventional techniques such as thermal gravimetric analysis (TGA). The results indicate that the combination of Cu, Ce, Ag, and Co catalysts has the best performance for low-temperature soot oxidation in both the HT and conventional experiments [26]. Despite the fast response time of IR thermography in the preliminary screening of catalytic activities, the chemical composition of the products formed during the reaction cannot be determined, which inhibits a wide applicability of the technique [24–31].

Like IR thermography, CTL has been applied to screen exothermic reactions, such as the catalytic oxidation of combustible gases [32]. The mechanism of CTL relies on detecting the chemiluminescence emissions of a combustion reaction occurring on a catalyst surface. The CTL intensity can be correlated with the catalyst activity [33]. Na et al. adapted CTL-based array imaging to monitor the CO oxidation activity of Au- and Pt-supported TiO_2 catalysts. One of the major advantages of CTL is that it can simultaneously provide a fast response time and evaluate the activity of catalysts at the temperature of interest. However, because the CTL responses of each catalyst are not known, the catalytic activity of metallic or bimetallic catalysts must be calibrated based on a second analysis technique such as gas chromatography (GC) or mass spectrometry (MS) [32].

LIFI is another optical technique that has been applied to HT catalyst screening. The principle of LIFI relies on the destruction or creation of chemical bonds that modify the florescence properties of the molecule. As the Ar^+ laser sheet irradiates the area above the catalyst, the change in the fluorescence intensity of products and unreacted species over the catalyst is detected by a charge-coupled device (CCD) camera, which can provide both IR thermography and florescence detection. Unlike IR thermography, the florescence intensity of species is linearly correlated and could provide information about the relative activity change of a particular reaction. Su et al. have employed LIFI and IR thermography in the HT screening of binary vanadia-based catalysts for naphthalene oxidation. They have shown that a library consisting of 15 catalysts can be screened *in situ* in 15 s. Due to their nature, only fluorescent species can be detected using LIFI. In addition, the signal-to-noise ratio (SNR) is inversely proportional to temperature due to increased blackbody emissions at high temperatures [34, 35].

While the aforementioned optical techniques utilize truly parallel HT approaches, REMPI spectroscopy has been used in HTE in a sequential manner using automation approaches [13, 36, 37]. In REMPI, a tunable ultraviolet (UV) laser beam is used to ionize reaction products, which are detected through an array of microelectrodes. This technique allows the researcher to analyze polyatomic molecules and radicals, and to distinguish isomers *in situ* in the parts-per-billion range. One of the drawbacks of this technique is that the suitable laser frequency for many molecules is unknown, limiting the applicability of this technique to catalyst screening [36, 37]. Senkan and Ozturk combined REMPI with microchannel array reactors to screen the dehydrogenation of cyclohexane to benzene [37]. In total, 66 ternary combinations of Pt, Pd, and In supported on alumina were tested in less than 5 h.

MS is a well-developed methodology that can be applied to HT screening in order to analyze complex gas mixtures in a sequential manner. Cong et al. utilized MS to investigate

the catalytic oxidation and reduction activity of 120 noble-metal catalysts, deposited by radiofrequency sputtering onto a quartz wafer. The samples were individually exposed to a gas mixture through a custom-designed probe. Both reactants and products were sampled directly above the catalyst and transferred to the mass spectrometer. Each sample was analyzed sequentially within a minute. Through this approach, the researchers analyzed a 136-catalyst library in less than 2.5 h [38]. Similarly, Senkan et al. coupled microreactor arrays with capillary microprobe sampling and quadrupole MS. The samples were analyzed in a sequential manner by inserting the probe into each microreactor channel. The analysis time required for each microreactor channel was reduced to 5 s, which allowed the screening of 80 microreactor channels in about 10 min [39]. Wang et al. also proposed MS for the analysis of effluent gas sampled through 80 reactors. Each reactor was connected to a stainless-steel capillary tube and individually selected for analysis via an automated 80-stream valve. The reactor effluent was transferred through a common sample port for analysis, with a sampling time of 8 s [40]. Although the sequential mode is typically fast enough to allow the researcher to obtain time-on-stream data, rapid deactivation processes may not be detected with this methodology. Richter et al. have applied time-of-flight MS to screen catalysts that are suitable for the selective catalytic reduction (SCR) of NO_x by hydrocarbons under lean exhaust conditions. In order to partially separate the reaction species, that is, NO, N_2, N_2O, CO, CO_2, and propane, from each other, GC has been coupled with time-of-flight MS. Reaction species coming from the 64-channel reactor were sequentially analyzed, while all channels were permanently on-stream. The entire library of 64 channels can be analyzed in 2.5 h [41].

GC is another versatile characterization technique that has been implemented to screen heterogeneous catalysts [42–49]. For example, Hoffmann et al. designed a 49-channel reactor for the parallelized HT screening of methane oxidization catalysts [44]. The reactors (inner diameter of 0.2 in, length of 0.71 in) were placed inside the bore of a stainless-steel flange. Gas was injected through a common inlet and passed through a diffuser plate to prevent back-mixing. Two GC setups, including a hot column and a cold column, were connected to a multiport valve via capillary tubes that were attached to the exit of each reaction channel. Using this setup, 42 different catalysts were sequentially analyzed for methane oxidation at two different temperatures in three days [44]. In addition, fast serial GC was used for the primary and secondary screening of oxidants for the direct amination of benzene to aniline [42]. A total of 25 000 samples per year were screened via a 24-parallel-batch reactor at high pressure. In our group, GC-MS was applied to the sequential screening of catalysts for the catalytic cracking of JP-8 in an HT reactor system consisting of a 16-channel reactor [12, 47]. The reactant gas feed is split into capillaries for flow equalization and then individually separated to reactor channels. Unreacted JP-8 and other hydrocarbons that exist in the liquid phase at room temperature are removed from each reactor effluent in a 16-channel parallel heat-exchange condenser. Product composition is then sequentially analyzed via GC-MS. Throughout the project, more than 100 catalyst samples were screened in less than six months and scaled up for the prototype development.

The major drawback in the application of GC to HTE is the necessarily long sampling time, which ultimately limits the usefulness of this technique in catalyst deactivation studies and kinetic studies. One possible solution for screening multiple catalysts in real time is to apply a multiplexing methodology to HTE. Multiplexing has been successfully applied to spectroscopy to enhance the duty cycle and SNR [48–52]. Trapp has applied this methodology to GC for the HT screening of effluents [48, 49]. In Trapp's HTE approach, samples are continuously admitted to GC by a six-port multiplexing injector through a pseudo-random sequence. The multiplexed chromatogram involves overlapped chromatograms of all the analytes sampled from different reactors. A Hadamard matrix is applied to deconvolute the time-shifted chromatogram of each analyte. The retention times, peak widths, and peak shapes of the analytes are determined in order to calculate the actual concentration of each sample. Multiple reactors can be connected to the multiplexing injector and effluents are pulsed to the GC in milliseconds, decreasing the overall sampling time significantly. Using an HT multiplexing GC, one can sample up to 453 samples per hour with a time-bin interval of 600 ms. In both sequential and parallel analyses of GC spectra, multiple-channel electronic valves are typically used at the exit of the reactors to select the particular flow for analysis. This type of valve is limited in temperature, preventing its usage for high-boiling-point effluents.

3 Application of FTIR parallel imaging

Two major advances in FTIR instrumentation over the past 20 years have enabled its use as an HT screening tool in heterogeneous catalysis. First, the incorporation of focal-plane array (FPA) detectors introduced an instrumental multiplex advantage that was previously absent in conventional FTIR systems. This advance facilitated the simultaneous collection of spatial and spectral information, limited only by the number of pixels on the FPA [53].

Second, the collection time for FTIR imaging data was reduced by an order of magnitude by replacing the commonly used step-scan spectrometer with a rapid-scanning spectrometer. Step-scan spectrometers typically achieve adequate SNR by collecting several frames of light-intensity information at each mirror retardation. These frames are then averaged to provide each interferogram point. In the rapid-scanning spectrometer scheme, data is collected continuously over the range of mirror retardations and requires only a single frame per interferogram point. In this way, the stabilizing time required for the mirror is avoided and the total acquisition time is reduced [54–57].

A setup composed of the asynchronous rapid-scanning FTIR spectrometer and FPA detector was first realized and demonstrated in our group as a viable parallel imaging technique for multi-channel reactors [54–58]. The basic concept of applying FTIR imaging to HT screening involves collecting

thousands of interferograms simultaneously using the FPA detector, which significantly decreases the time required to acquire an FTIR image. For example, a spectral image with 4 cm^{-1} spectral resolution and a spectral range of 1360 cm^{-1} can be collected in only 34 s. Such an image will contain a total of 12 384 spectra, based on a 128 × 128 FPA detector [56].

Since its development, the HT-FTIR system has facilitated numerous studies within our group. A notable example was the optimization and development of alumina-supported Pt, Ba, and Fe containing NO_x storage and reduction catalysts over a wide parameter space including catalyst composition, feed composition, cycling conditions, and transition-metal promoters. These studies led to the discovery of Co/Ba as a highly effective and noble-metal-free NO_x storage catalyst [59–61]. Additional HT studies focused on the micro kinetics of ammonia decomposition [62], the stability of small pore zeolites in the NH_3-SCR of NO_x [63], promotional effects for Ag-catalyzed ethylene epoxidation [64, 65], and several other topics [66, 67].

The pioneering design of the HT-FTIR screening influenced other researchers. Kubanek et al. have improved the degree of parallelization and designed a 49-channel reactor implemented in a FPA-IR setup [68]. The gaseous reaction mixture is introduced through one common inlet and split into each reactor via a capillary bundle. The effluent gas from the reactors is introduced directly into the analysis capillaries, in which the compositions of the effluents are analyzed simultaneously by IR spectroscopy. The activity of different catalysts for *n*-pentane hydroisomerization was reported with a relative error of less than ± 20% [68]. Furthermore, Chan et al. adapted the HT imaging approach to screen aqueous solutions and samples in contact with water using micro-attenuated total reflection (ATR) imaging [69–72]. They have employed a single reflection diamond ATR accessory in connection with a 64 × 64 FPA detector, which allows IR spectra to be measured with a small amount of sample at a variety of temperatures. Due to the durability of the diamond ATR accessory, high pressure can be applied to improve the contact between the samples and crystal, thereby reducing the absorbance variations for the measurement. Using this setup, 40 samples of ibuprofen in polyethylene glycol formulations were screened and the specific weight fraction of ibuprofen in polyethylene glycol was determined in order to avoid its dimerization [72].

In summary, rapid-scanning FTIR imaging has proven to be an effective parallel characterization method as demonstrated by the diverse sets of HT reaction studies carried out over the last decade, both within our group and by other researchers. FTIR can be used to identify gaseous and liquid species in the mid-IR range and to quantify gas-phase concentrations in a univariate or multivariate manner. The major limitation of HT-FTIR is its applicability only to IR-active molecules.

4 16-channel HT reactor designs

The first generation of a 16-channel reactor was designed in a honeycomb block structure that included an equal number of heater and reactor blocks (Figure 1(a)) [73]. The second generation of our 16-channel parallel plug-flow reactor marks several improvements over the first, including a more efficient catalyst loading/unloading process, improved temperature control, and an improved flow-distribution system. In lieu of heating blocks, four ceramic radiant heaters (with an inner diameter of 3 in and a height of 6 in) are used for the new design (Figure 1(b)). Ceramic vestibules fit snugly into the top and bottom of each furnace for optimum insulation of the heated area. Since channel temperatures are controlled in groups of 4 rather than 16, improved temperature distribution is achieved, in addition to the flexibility of running four different reaction temperatures simultaneously. Four on-off proportional-integral-derivative (PID) controllers are used to control the power to each of the four furnaces, based on temperature readings from K-type thermocouples placed in the center of each furnace. These temperatures are displayed on an in-house-developed LabView® program alongside the 16 measured catalyst-bed temperatures.

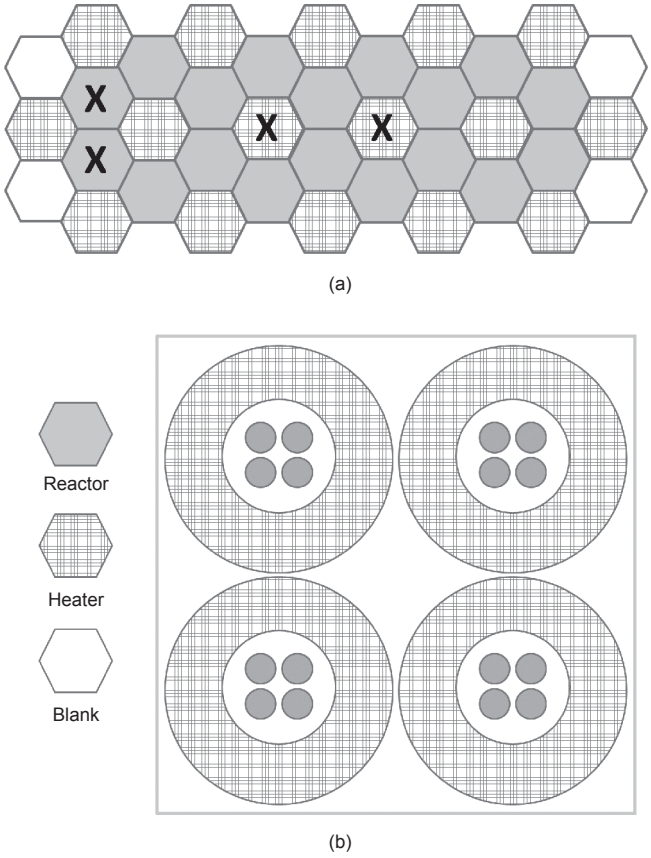

Figure 1. The HT reactor. (a) First generation; (b) second generation.

The 16-channel reactor apparatus, shown in Figure 2, features a stationary bottom plate and a moving top plate, which can be lifted with a small winch system to quickly load and unload catalysts. Typically, reactor tubes are preloaded with between 50 mg and 500 mg of powdered catalyst, supported on stainless-steel frits. The movable top plate is then lowered to meet the reactor tubes. Flow is distributed equally among the 16 channels using a network of concentric capillary spirals stemming from a central inlet line, all contained inside a heated box. The outlets of this capillary box serve as the

inlets to the 16 parallel fixed-bed reactors. For clarity, Figure 2 does not include the heated areas and the additional 15 reactor channels.

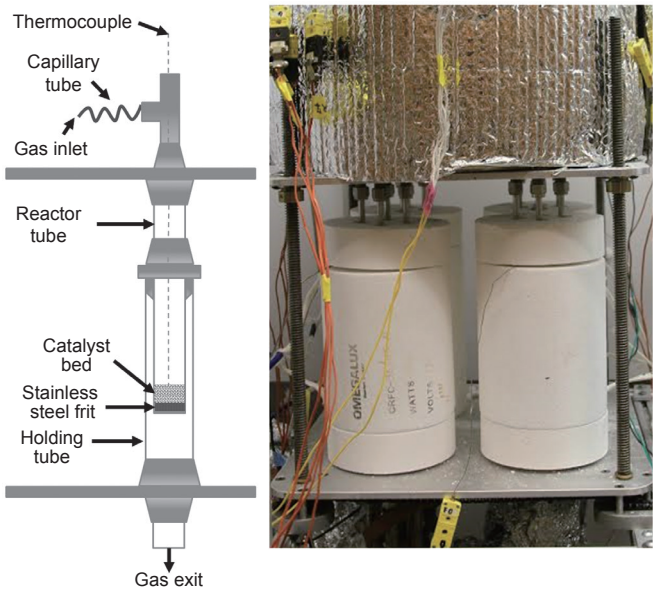

Figure 2. 16-channel HT reactor. Individual reactor design is shown on the left.

The HT-FTIR experimental setup (Figure 3) is comprised of a Bruker Equinox 55 FTIR spectrometer and a 128 × 128 pixel mercury cadmium telluride FPA detector (Santa Barbara Focalplane, Goleta, CA, USA) operated at 1610 Hz and sensitive in the range of 4000–1000 cm^{-1}. Spectra are typically taken with 8 cm^{-1} spectral resolution. A set of refractive optical elements were paired with an in-house-developed gas-phase array (GPA) sampling accessory [74]. Further details can be found in Refs. [54–58]. The optical elements include a gold-plated front-surface mirror, two ZnSe meniscus lenses for beam spreading, and two plano-convex BaF_2 lenses for beam collimation. Between the two sets of lenses, the beam travels through the GPA sampling accessory, which is comprised of a bundle of 16 stainless-steel tubes (outside diameter of 3/8 in). Each end of the GPA is capped with 1.97 in × 0.12 in ZnSe windows sealed with O-rings. The effluent gases from 16 reactor channels enter and exit the GPA through 1/8 in tubing welded to the GPA tubes.

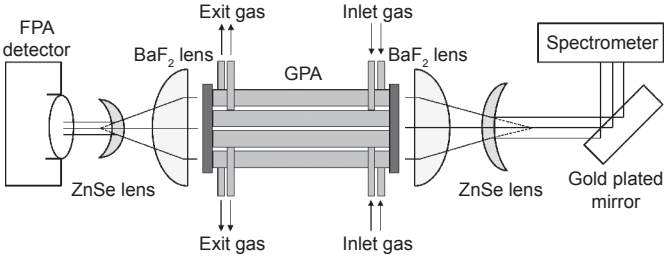

Figure 3. FTIR parallel imaging apparatus [66].

Data acquisition is controlled via an in-house-written software. Each interferogram contains 3554 data points. The data collection process for one spectral image containing 128 × 128 interferograms at a FPA frame rate of 1610 Hz takes approximately 2 s. In order to improve the SNR, typically 32 interferograms are collected and averaged in under a minute. Subsequent data processing including the elimination of bad pixels and the Fourier transform of the signal is performed using an in-house-developed software package [74]. Quantitative analysis of the resultant multichannel IR spectra proceeds analogously to that of traditional IR and can be performed in a matter of seconds using GRAMS/AI calibration and prediction software [75] to yield effluent gas-phase concentrations.

5 Case study: CO oxidation over cobalt oxide catalysts

A case study has been conducted to show that rapid-scanning FTIR coupled with the HT reactor can be used to resolve even small differences in catalyst performance introduced by varying synthesis conditions. We briefly discuss how the DOE was paired with HTE to study the influence of six synthesis conditions on the CO oxidation activity of unsupported cobalt oxide nanoparticles. In total, the performance of 29 unique cobalt oxide catalysts was evaluated in less than two days. Paired with the relative efficiency of a six-factor designed experiment over its one-factor-at-a-time analog, the total experimental time was decreased by a factor of 50.

The cobalt catalyst library was prepared via the hydrothermal reduction of cobalt acetate with 1,2-dodecanediol. Synthesis parameters reported in the literature to influence the size, morphology, and crystal structure of cobalt nanoparticles prepared with this method were varied at levels representative of the entire design space [76, 77]. Specifically, the synthesis was carried out using 0.05–0.15 $mol \cdot L^{-1}$ cobalt acetate and 0.05–0.25 $mol \cdot L^{-1}$ of either polyvinyl pyrrolidone (PVP) or oleic acid surfactants in 30 mL of dibenzyl ether, at a temperature of 240–270 °C and a ramp rate of 1–10 $°C \cdot min^{-1}$, using reducer-reductant molar ratios from 2 to 8 (Table 1). Factorial design of the experiments was employed in order to systematically study these factors [78], and X-ray diffraction studies were carried out to resolve the influence of the factors on the bulk crystal structure of the particles. The crystalline phase was determined for each sample based on the relationship between lattice parameters, miller indices, and d-spacing for cobalt, and Scherrer equation was applied to approximate crystallite size from peak broadening [79, 80]. Prior to catalytic testing, all samples were dried at 110 °C and calcined at 550 °C for 14 h in air to ensure complete oxidation to the spinel structure, Co_3O_4. The post-calcination cobalt oxide grain sizes ranged from 32 nm to 100 nm, as shown in Table 1.

A preliminary CO oxidation benchmark study was completed to quantify the overall measurement error associated with the 16-channel apparatus. A mixture of 2% CO and 5% O_2 balanced with N_2 was injected into each channel at a target space velocity of 60 000 $mL \cdot h^{-1} \cdot g_{cat}^{-1}$ over a temperature ramp of 100–300 °C. Each channel (except a single blank channel) was loaded with 100 mg of commercial 1% Pd/Al_2O_3 catalyst

Table 1. Synthesis conditions of Co_3O_4 catalysts tested.

No.	Synthesis temperature (°C)	Ramp rate (°C·min^{-1})	Concentration of surfactant (mol·L^{-1})	Metal salt (mol·L^{-1})	*R*: Reducer/Co mole ratio	Surfactant	Grain size (nm)	T_{50} (°C)	Activity at 200 °C (mL·(g-s)$^{-1}$)
1	240	1	0.05	0.15	8	PVP	37	194	0.47
2	270	1	0.05	0.05	2	PVP	48	185	1.12
3	240	10	0.05	0.05	8	OA	49	203	0.72
4	270	10	0.05	0.15	2	OA	48	165	0.47
5	240	1	0.25	0.15	2	OA	48		0.09
6	270	1	0.25	0.05	8	OA	55	168	1.18
7	270	10	0.25	0.15	8	PVP	49	178	0.61
8	240	1	0.05	0.05	8	PVP	42	178	1.42
9	270	1	0.05	0.15	2	PVP		231	1.54
10	240	10	0.05	0.15	8	OA	58	158	0.26
11	270	10	0.05	0.05	2	OA	58	141	0.18
12	240	1	0.25	0.05	2	OA	49	179	1.28
13	270	1	0.25	0.15	8	OA	82	203	0.27
14	240	10	0.25	0.15	2	PVP	49	172	0.31
15	270	10	0.25	0.05	8	PVP	46	151	0.38
16	255	5.5	0.15	0.1	5	OA	60	144	0.56
17	255	5.5	0.15	0.1	5	PVP	34	197	0.89
18	240	1	0.05	0.15	2	PVP	> 100	212	0.63
19	270	10	0.05	0.15	8	OA	32	123	0.31
20	270	1	0.25	0.05	2	OA	53	142	0.21
21	240	10	0.25	0.05	8	PVP	68	160	0.46
22	270	10	0.25	0.15	2	PVP	49	197	0.95
23	240	1	0.05	0.05	2	PVP	64.7	119	0.58
24	270	1	0.05	0.15	8	PVP	58	162	0.43
25	240	10	0.05	0.15	2	OA	47	172	1.72
26	270	10	0.05	0.05	8	OA	54	160	0.53
27	270	1	0.25	0.15	2	OA		302	1.09
28	240	10	0.25	0.15	8	PVP	60	146	1.69
29	255	5.5	0.15	0.1	5	OA	76	192	0.55

Note: OA—oleic acid.

(Alfa Aesar). Both flow and temperature distributions were uniform across the 16 channels with relative standard errors of ± 1.3% and ± 0.7%, respectively. Above 200 °C, all the channels containing Pd/Al_2O_3 showed uniform conversions with a relative standard error of ± 3.5%. All standard errors were calculated on a 95% confidence interval.

CO oxidation activity tests for the Co_3O_4 nanoparticles were carried out using 50 mg of catalyst per channel under a 2% CO/8% O_2/N_2 gas stream at a space velocity of 60 000 mL·h^{-1}·g$_{cat}^{-1}$. The reactor effluent composition was measured via FTIR at intervals of 25 °C between 25 °C and 300 °C. Time on stream was 30 min per temperature, with ramp-up and stabilization between temperatures requiring less than 10 min. Catalyst-bed temperatures were measured for each channel and used in subsequent calculations. Again, a single channel was left empty of catalytic material in each experiment to ensure zero conversion of the empty reactor tubes. All catalytic activities were tested under atmospheric pressure. The synthesis conditions of each catalyst tested are listed in Table 1.

In a typical experiment, several IR spectral images were taken at each temperature point and averaged to improve the SNR of the spectra. Subsequently, univariate calibrations were applied to quantify both the CO and CO_2 outlet concentrations from the IR pathlength and the absorbance of the CO and CO_2 vibrational bands. In all cases, the carbon balance over the conditions studied was closed within ± 1.5%. From this information, catalytic activities were calculated in the range from 0.09 ± 0.003 to 1.72 ± 0.06 mL·(g-s)$^{-1}$, taking into account the precise catalyst mass, flow rate, and CO converted in each channel. Light-off temperatures (T_{50}) at 50% CO conversion ranged from 119 °C to 302 °C.

The results were used to develop a predictive model correlating the aforementioned cobalt synthesis parameters with CO oxidation activity at 200 °C. Factorial analysis and model regression were performed using Minitab statistical software [81]. Specifically, 23 of the Co_3O_4 catalysts tested with the HT system were used to fit the statistical model, while the remaining 6 were used for validation. Only terms with a $P < 0.05$ were included in the statistical model. It has been found that cobalt concentration, surfactant concentration, and surfactant type are the most significant main effects. Further analysis of the significant two-way interaction effect for ramp rate and temperature showed that increasing ramp rate positively influences activity at low synthesis temperatures, but has an opposite influence at high synthesis temperatures. This interaction is shown in the contour map in Figure 4.

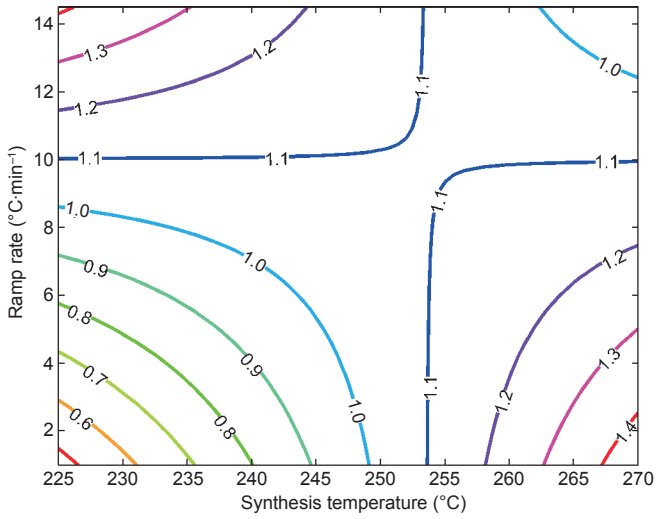

Figure 4. Contour plot obtained from statistical model. CO oxidation activity at 200 °C (mL·(g-s)$^{-1}$). The hold values were 0.05 mol·L^{-1} of surfactant concentration, 0.1 mol·L^{-1} of cobalt concentration, $R = 2$ of molar ratio, and PVP.

The predictive ability of the statistical model is shown in Figure 5. The predicted activity of the model development points and validation points matched well with the experimental activity. Model reproducibility was evaluated by carrying out repeated synthesis and catalytic testing on several design points (validating data points). Between replicates, differences ranged from 0.41% to 6.39% and did not change the predictive model appreciably. This result demonstrates the usefulness of the HT system in resolving the changes in catalytic performance produced by the breadth of the synthesis conditions studied.

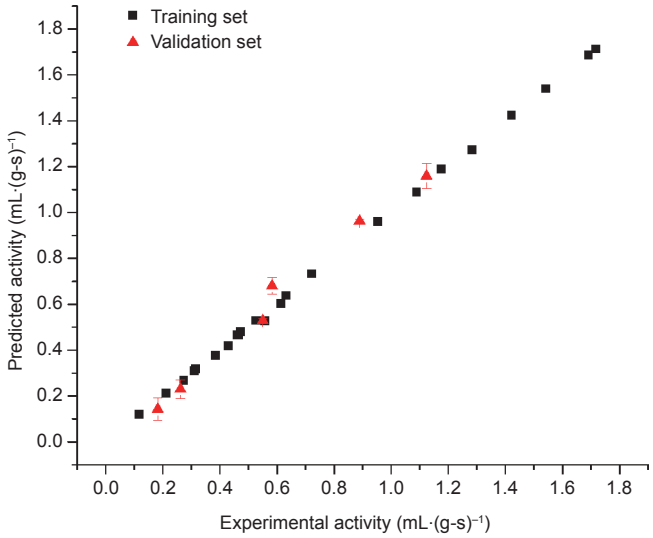

Figure 5. Comparison of predicted activity with experimental activity.

6 Conclusions

HTE can dramatically improve catalyst discovery, development, and deployment. Over the years, many HT screening techniques have been utilized to evaluate the activity of catalysts in a parallel fashion. Among these techniques, rapid-scanning HT-FTIR imaging was first proposed in our group almost two decades ago and was applied successfully to screen heterogeneous catalysts for many applications including NH_3 decomposition, SCR of NO_x, and ethylene epoxidation.

Here, we report the new design of the 16-channel HT reactor and FTIR system. The performance of the system was rigorously tested for accuracy and reproducibility. The system was shown to exhibit nearly uniform flow rates, gas compositions, and heating profiles across all channels. Reaction results were found to be reproducible over both single-catalyst and multiple-catalyst studies, with an overall error of ± 3.5%. The activity of cobalt oxide nanoparticles for CO oxidation was measured and a statistical model was developed to correlate synthesis parameters to the activity.

The factorial analysis of CO oxidation on cobalt oxides proved useful in probing the synthesis parameter design space and in directing future studies. An accurate and reproducible model correlating Co_3O_4 synthesis parameters with CO oxidation activity was quickly formulated by pairing DOE with the HT reactor and rapid-scanning FTIR system. Several regions of interests have been investigated, with the most promising being the high/low combinations of the synthesis temperature/ramp rate interaction. In the future, the model will be further validated by testing points outside of the range studied and a response surface study will be conducted in order to reach a full understanding of the underlying complexities.

Acknowledgement

The authors acknowledge the South Carolina SmartState Center for Strategic Approaches to the Generation of Electricity (SAGE) for funding.

Compliance with ethics guidelines

Erdem Sasmaz, Kathleen Mingle, and Jochen Lauterbach declare that they have no conflict of interest or financial conflicts to disclose.

References

1. Anon. Recognizing the best in innovation: Breakthrough catalyst. *R&D Magazine*, 2005, September: 20
2. M. Baerns, M. Holeňa. Approaches in the development of heterogeneous catalysts. In: M. Baerns, M. Holeňa, eds. *Combinatorial Development of Solid Catalytic Materials: Design of High-Throughput Experiments, Data Analysis, Data Mining*. London: Imperial College Press, 2009: 7–20
3. A. Jain, et al. Commentary: The Materials Project: A materials genome approach to accelerating materials innovation. *APL Mat.*, 2013, 1(1): 011002
4. H. Shibata, et al. Heterogeneous catalysis high throughput workflow: A case study involving propane oxidative dehydrogenation. In: A. Hagemeyer, A. F. Volpe Jr., eds. *Modern Applications of High Throughput R&D in Heterogeneous Catalysis*. Sharjah: Bentham Science Publishers, 2014: 173–196
5. H. W. Turner, A. F. Volpe Jr., W. H. Weinberg. High-throughput heterogeneous catalyst research. *Surf. Sci.*, 2009, 603(10–12): 1763–1769
6. I. E. Maxwell, P. van den Brink, R. S. Downing, A. H. Sijpkes, S. Gomez,

Th. Maschmeyer. High-throughput technologies to enhance innovation in catalysis. *Top. Catal.*, 2003, 24(1–4): 125–135
7. W. F. Maier, K. Stöwe, S. Sieg. Combinatorial and high-throughput materials science. *Angew. Chem. Int. Ed. Engl.*, 2007, 46(32): 6016–6067
8. D. Farrusseng. High-throughput heterogeneous catalysis. *Surf. Sci. Rep.*, 2008, 63(11): 487–513
9. R. Potyrailo, K. Rajan, K. Stoewe, I. Takeuchi, B. Chisholm, H. Lam. Combinatorial and high-throughput screening of materials libraries: Review of state of the art. *ACS Comb. Sci.*, 2011, 13(6): 579–633
10. J. P. Holdren. *Materials Genome Initiative for Global Competitiveness*. Washington, DC: National Science and Technology Council, 2011
11. D. D. Devore, R. M. Jenkins. Impact of high throughput experimentation on homogeneous catalysis research. *Comment. Inorg. Chem.*, 2014, 34(1–2): 17–41
12. J. Lauterbach, E. Sasmaz, J. Bedenbaugh, S. Kim, J. Hattrick-Simpers. Discovery and optimization of coking and sulfur resistant Bi-metallic catalyst for cracking JP-8: From thin film libraries to single powders. In: A. Hagemeyer, A. F. Volpe Jr., eds. *Modern Applications of High Throughput R&D in Heterogeneous Catalysis*. Sharjah: Bentham Science Publishers, 2014: 89–117
13. S. Senkan. Combinatorial heterogeneous catalysis—A new path in an old field. *Angew. Chem. Int. Ed. Engl.*, 2001, 40(2): 312–329
14. J. R. Ebner, M. R. Thompson. An active site hypothesis for well-crystallized vanadium phosphorus oxide catalyst systems. *Catal. Today*, 1993, 16(1): 51–60
15. R. Schlögl. Combinatorial chemistry in heterogeneous catalysis: A new scientific approach or "the King's New Clothes"? *Angew. Chem. Int. Edit.*, 1998, 37(17): 2333–2336
16. U. Rodemerck, M. Baerns, M. Holena, D. Wolf. Application of a genetic algorithm and a neural network for the discovery and optimization of new solid catalytic materials. *Appl. Surf. Sci.*, 2004, 223(1–3): 168–174
17. J. M. Caruthers, et al. Catalyst design: Knowledge extraction from high-throughput experimentation. *J. Catal.*, 2003, 216(1–2): 98–109
18. Y. Yang, T. Lin, X. L. Weng, J. A. Darr, X. Z. Wang. Data flow modeling, data mining and QSAR in high-throughput discovery of functional nanomaterials. *Comput. Chem. Eng.*, 2011, 35(4): 671–678
19. A. G. Maldonado, G. Rothenberg. Predictive modeling in catalysis—From dream to reality. *Chem. Eng. Prog.*, 2009, 105(6): 26–32
20. G. Rothenberg. Data mining in catalysis: Separating knowledge from garbage. *Catal. Today*, 2008, 137(1): 2–10
21. J. M. Serra, A. Corma, A. Chica, E. Argente, V. Botti. Can artificial neural networks help the experimentation in catalysis? *Catal. Today*, 2003, 81(3): 393–403
22. J. M. Serra, A. Corma, E. Argente, S. Valero, V. Botti. Neural networks for modelling of kinetic reaction data applicable to catalyst scale up and process control and optimisation in the frame of combinatorial catalysis. *Appl. Catal. A Gen.*, 2003, 254(1): 133–145
23. H. U. Gremlich. The use of optical spectroscopy in combinatorial chemistry. *Biotechnol. Bioeng.*, 1998/1999, 61(3): 179–187
24. S. Schmatloch, M. A. R. Meier, U. S. Schubert. Instrumentation for combinatorial and high-throughput polymer research: A short overview. *Macromol. Rapid Comm.*, 2003, 24(1): 33–46
25. Y. Zhang, X. Gong, H. Zhang, R. C. Larock, E. S. Yeung. Combinatorial screening of homogeneous catalysis and reaction optimization based on multiplexed capillary electrophoresis. *J. Comb. Chem.*, 2000, 2(5): 450–452
26. N. E. Olong, K. Stöwe, W. F. Maier. A combinatorial approach for the discovery of low temperature soot oxidation catalysts. *Appl. Catal. B Environ.*, 2007, 74(1–2): 19–25
27. F. C. Moates, M. Somani, J. Annamalai, J. T. Richardson, D. Luss, R. C. Willson. Infrared thermographic screening of combinatorial libraries of heterogeneous catalysts. *Ind. Eng. Chem. Res.*, 1996, 35(12): 4801–4803
28. A. Holzwarth, H. W. Schmidt, W. F. Maier. Detection of catalytic activity in combinatorial libraries of heterogeneous catalysts by IR thermography. *Angew. Chem. Int. Edit.*, 1998, 37(19): 2644–2647
29. C. Brooks, et al. High throughput discovery of CO oxidation/VOC combustion and water-gas shift catalysts for industrial multi-component streams. *Top. Catal.*, 2006, 38(1–3): 195–209
30. S. J. Taylor, J. P. Morken. Thermographic selection of effective catalysts from an encoded polymer-bound library. *Science*, 1998, 280(5361): 267–270
31. J. Klein, et al. Accelerating lead discovery via advanced screening methodologies. *Catal. Today*, 2003, 81(3): 329–335
32. N. Na, S. Zhang, X. Wang, X. Zhang. Cataluminescence-based array imaging for high-throughput screening of heterogeneous catalysts. *Anal. Chem.*, 2009, 81(6): 2092–2097
33. M. Breysse, B. Claudel, L. Faure, M. Guenin, R. J. J. Williams. Chemiluminescence during the catalysis of carbon monoxide oxidation on a thoria surface. *J. Catal.*, 1976, 45(2): 137–144
34. H. Su, E. S. Yeung. High-throughput screening of heterogeneous catalysts by laser-induced fluorescence imaging. *J. Am. Chem. Soc.*, 2000, 122(30): 7422–7423
35. H. Su, Y. Hou, R. S. Houk, G. L. Schrader, E. S. Yeung. Combinatorial screening of heterogeneous catalysis in selective oxidation of naphthalene by laser-induced fluorescence imaging. *Anal. Chem.*, 2001, 73(18): 4434–4440
36. S. M. Senkan. High-throughput screening of solid-state catalyst libraries. *Nature*, 1998, 394(6691): 350–353
37. S. M. Senkan, S. Ozturk. Discovery and optimization of heterogeneous catalysts by using combinatorial chemistry. *Angew. Chem. Int. Edit.*, 1999, 38(6): 791–795
38. P. Cong, et al. High-throughput synthesis and screening of combinatorial heterogeneous catalyst libraries. *Angew. Chem. Int. Edit.*, 1999, 38(4): 483–488
39. S. Senkan, K. Krantz, S. Ozturk, V. V. Zengin, I. I. Onal. High-throughput testing of heterogeneous catalyst libraries using array microreactors and mass spectrometry. *Angew. Chem. Int. Ed. Engl.*, 1999, 38(18): 2794–2799
40. H. Wang, Z. Liu, J. Shen. Quantified MS analysis applied to combinatorial heterogeneous catalyst libraries. *J. Comb. Chem.*, 2003, 5(6): 802–808
41. M. Richter, et al. Combinatorial preparation and high-throughput catalytic tests of multi-component deNO$_x$ catalysts. *Appl. Catal. B Environ.*, 2002, 36(4): 261–277
42. A. Hagemeyer, et al. Application of combinatorial catalysis for the direct amination of benzene to aniline. *Appl. Catal. A Gen.*, 2002, 227(1–2): 43–61
43. S. Gomez, J. A. Peters, J. C. van der Waal, T. Maschmeyer. High-throughput experimentation as a tool in catalyst design for the reductive amination of benzaldehyde. *Appl. Catal. A Gen.*, 2003, 254(1): 77–84
44. C. Hoffmann, H. W. Schmidt, F. Schüth. A multipurpose parallelized 49-channel reactor for the screening of catalysts: Methane oxidation as the example reaction. *J. Catal.*, 2001, 198(2): 348–354
45. M. Lucas, P. Claus. High throughput screening in monolith reactors for total oxidation reactions. *Appl. Catal. A Gen.*, 2003, 254(1): 35–43
46. C. Kiener. High-throughput screening under demanding conditions: Cu/ZnO catalysts in high pressure methanol synthesis as an example. *J. Catal.*, 2003, 216(1–2): 110–119
47. J. E. Bedenbaugh, S. Kim, E. Sasmaz, J. Lauterbach. High-throughput investigation of catalysts for JP-8 fuel cracking to liquefied petroleum gas. *ACS Comb. Sci.*, 2013, 15(9): 491–497
48. O. Trapp. Boosting the throughput of separation techniques by "multiplex-

ing". *Angew. Chem. Int. Ed. Engl.*, 2007, 46(29): 5609–5613
49. O. Trapp. Gas chromatographic high-throughput screening techniques in catalysis. *J. Chromatogr. A*, 2008, 1184(1–2): 160–190
50. R. R. Ernst, W. A. Anderson. Application of Fourier transform spectroscopy to magnetic resonance. *Rev. Sci. Instrum.*, 1966, 37(1): 93–102
51. M. B. Comisarow, A. G. Marshall. Fourier transform ion cyclotron resonance spectroscopy. *Chem. Phys. Lett.*, 1974, 25(2): 282–283
52. O. Trapp, J. R. Kimmel, O. K. Yoon, I. A. Zuleta, F. M. Fernandez, R. N. Zare. Continuous two-channel time-of-flight mass spectrometric detection of electrosprayed ions. *Angew. Chem. Int. Ed. Engl.*, 2004, 43(47): 6541–6544
53. E. N. Lewis, et al. Fourier transform spectroscopic imaging using an infrared focal-plane array detector. *Anal. Chem.*, 1995, 67(19): 3377–3381
54. C. M. Snively, G. Oskarsdottir, J. Lauterbach. Chemically sensitive high throughput parallel analysis of solid phase supported library members. *J. Comb. Chem.*, 2000, 2(3): 243–245
55. C. M. Snively, G. Oskarsdottir, J. Lauterbach. Parallel analysis of the reaction products from combinatorial catalyst libraries. *Angew. Chem. Int. Ed. Engl.*, 2001, 40(16): 3028–3030
56. C. M. Snively, S. Katzenberger, G. Oskarsdottir, J. Lauterbach. Fourier-transform infrared imaging using a rapid-scan spectrometer. *Opt. Lett.*, 1999, 24(24): 1841–1843
57. C. M. Snively, G. Oskarsdottir, J. Lauterbach. Chemically sensitive parallel analysis of combinatorial catalyst libraries. *Catal. Today*, 2001, 67(4): 357–368
58. C. M. Snively, J. Lauterbach, M. Christopher. Sampling accessories for HTE of combinatorial libraries using spectral imaging. *Spectroscopy*, 2002, 17(4), 26–33
59. R. J. Hendershot, W. B. Rogers, C. M. Snively, B. Ogunnaike, J. Lauterbach. Development and optimization of NO_x storage and reduction catalysts using statistically guided high-throughput experimentation. *Catal. Today*, 2004, 98(3): 375–385
60. R. J. Hendershot, R. Vijay, C. M. Snively, J. Lauterbach. High-throughput study of the performance of storage and reduction catalysts as a function of cycling conditions and catalyst composition. *Chem. Eng. Sci.*, 2006, 61(12): 3907–3916
61. R. Vijay, et al. Noble metal free NO_x storage catalysts using cobalt discovered via high-throughput experimentation. *Catal. Commun.*, 2005, 6(2): 167–171
62. B. J. Feist. High throughput experimentation and microkinetic modeling (Master's thesis). Newark, DE: University of Delaware, 2006
63. D. W. Fickel, E. D'Addio, J. A. Lauterbach, R. F. Lobo. The ammonia selective catalytic reduction activity of copper-exchanged small-pore zeolites. *Appl. Catal. B Environ.*, 2011, 102(3–4): 441–448
64. J. C. Dellamorte, J. Lauterbach, M. A. Barteau. Effect of preparation conditions on Ag catalysts for ethylene epoxidation. *Top. Catal.*, 2010, 53(1–2): 13–18
65. J. C. Dellamorte, J. Lauterbach, M. A. Barteau. Palladium-silver bimetallic catalysts with improved activity and selectivity for ethylene epoxidation. *Appl. Catal. A Gen.*, 2011, 391(1–2): 281–288
66. E. D'Addio. High throughput Investigation of supported catalysts for CO_x-free hydrogen production from ammonia decomposition (Doctoral dissertation). Newark, DE: University of Delaware, 2011
67. S. Salim. Development of high-throughput catalyst screening for ammonia based selective catalytic reduction of nitric oxide with parallel analysis using Fourier transform infrared imaging (Master's thesis). Columbia, SC: University of South Carolina, 2013
68. P. Kubanek, O. Busch, S. Thomson, H. W. Schmidt, F. Schüth. Imaging reflection IR spectroscopy as a tool to achieve higher integration for high-throughput experimentation in catalysis research. *J. Comb. Chem.*, 2004, 6(3): 420–425
69. K. L. A. Chan, S. G. Kazarian. FTIR spectroscopic imaging of dissolution of a solid dispersion of nifedipine in poly(ethylene glycol). *Mol. Pharm.*, 2004, 1(4): 331–335
70. K. L. A. Chan, S. G. Kazarian. New opportunities in micro- and macro-attenuated total reflection infrared spectroscopic imaging: Spatial resolution and sampling versatility. *Appl. Spectrosc.*, 2003, 57(4): 381–389
71. K. L. A. Chan, S. G. Kazarian, A. Mavraki, D. R. Williams. Fourier transform infrared imaging of human hair with a high spatial resolution without the use of a synchrotron. *Appl. Spectrosc.*, 2005, 59(2): 149–155
72. K. L. A. Chan, S. G. Kazarian. High-throughput study of poly(ethylene glycol)/ibuprofen formulations under controlled environment using FTIR imaging. *J. Comb. Chem.*, 2006, 8(1): 26–31
73. R. J. Hendershot, et al. A novel reactor system for high throughput catalyst testing under realistic conditions. *Appl. Catal. A Gen.*, 2003, 254(1): 107–120
74. S. S. Lasko. Quantitative high-throughput studies of catalyst libraries (Master's thesis). West Lafayette, IN: Purdue University, 2002
75. Anon. GRAMS/AI^{TM} with PLSplus/IQ add-on. Waltham, MA: Thermo Fischer Scientific Inc., 2009
76. N. Wu, L. Fu, M. Su, M. Aslam, K. C. Wong, V. P. Dravid. Interaction of fatty acid monolayers with cobalt nanoparticles. *Nano Lett.*, 2004, 4(2): 383–386
77. C. Wen, X. Zhang, S. E. Lofland, J. Lauterbach, J. Hattrick-Simpers. Synthesis of mono-disperse CoFe alloy nanoparticles with high activity toward $NaBH_4$ hydrolysis. *Int. J. Hydrogen Energy*, 2013, 38(15): 6436–6441
78. D. C. Montgomery. *Design and Analysis of Experiments*. 3rd ed. Somerset, NJ: John Wiley & Sons, Inc., 1991
79. L. V. Azaroff, M. J. Buerger. *The Powder Method in X-Ray Crystallography*. New York: McGraw-Hill, 1958
80. N. F. M. Henry, H. Lipson, W. A. Wooster. *The Interpretation of X-Ray Diffraction Photographs*. London: MacMillon, 1961
81. Anon. Minitab 17 statistical software. State College, PA: Minitab, Inc., 2010